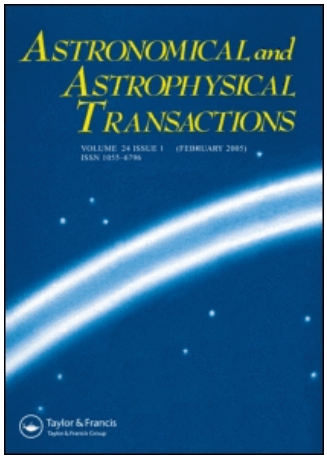


Astronomical & Astrophysical Transactions
The Journal of the Eurasian Astronomical Society
Publication details, including instructions for authors and subscription information:
http://www.informaworld.com/smpp/title~content=t713453505

# The correlation between the local density of luminous red galaxies and the presence of gamma-ray bursts

X. -F. Deng [a]; Y. -Q. Chen [b]; P. Jiang [a]; J. Song [a]
[a] Mathematics and Physics College, Nanchang University, Jiangxi, PR China
[b] Management College, Nanchang University, Jiangxi, PR China

Online Publication Date: 01 August 2006
To cite this Article: Deng, X. -F., Chen, Y. -Q., Jiang, P. and Song, J. (2006) 'The correlation between the local density of luminous red galaxies and the presence of gamma-ray bursts', Astronomical & Astrophysical Transactions, 25:4, 253 - 259
To link to this article: DOI: 10.1080/10556790601033015
URL: http://dx.doi.org/10.1080/10556790601033015

*Astronomical and Astrophysical Transactions*
Vol. 25, No. 4, August 2006, 253–259





# The correlation between the local density of luminous red galaxies and the presence of gamma-ray bursts

X.-F. DENG*†, Y.-Q. CHEN‡, P. JIANG† and J. SONG†

†Mathematics and Physics College, Nanchang University, Jiangxi 330047, PR China
‡Management College, Nanchang University, Jiangxi 330047, PR China

*(Received 11 November 2005)*

In order to explore the characteristics of the environment surrounding the gamma-ray bursts (GRBs), we have studied the correlation between the local density of luminous red galaxies (LRGs) and the presence of GRBs. Using the LRG sample in the Sloan Digital Sky Survey Data Release 3 (SDSS DR3) and the *Burst and Transient Source Experiment (BATSE) Current GRB Catalog*, we have calculated the local surface density of LRGs within an angular radius of less than 2° surrounding each burst in the *GRB Catalog*. The results show that there is no correlation between the local density of LRGs and the presence of GRBs.

*Keywords*: Gamma-ray bursts; Luminous red galaxies; Correlation

## 1. Introduction

The origin of cosmological gamma-ray bursts (GRBs) remains one of the great mysteries of modern astronomy [1]. Over the past half-decade, many advances have been made in understanding the nature of the bursts and their afterglows throughout the electromagnetic spectrum. The scenario for the origin of GRBs mainly consists of two sets of models. One set of models predicts that GRBs occur when two collapsed objects (such as black holes or neutron stars) merge [2, 3]. The other major set of models describes the fact that GRBs are associated with the death of massive stars (supernovae or hypernovae) [4–6].

The characteristics of the physical environment surrounding the bursts may provide strong constraints for the origin of these events. In the process of exploring the physical environment surrounding the bursts, it will be meaningful to study the correlation between the local density of galaxies and the presence of GRBs or the environment of GRB host galaxies. Fynbo *et al.* [7], studying the Ly$\alpha$ emission of two GRB fields (GRB 000301C and GRB 000926), found a number of galaxies at the same red shift of GRB hosts without signs of overdensity on small scales. Moreover, the lack of blank fields at a similar depth prevented these workers from concluding whether GRB hosts reside in overdense regions. From an

*Corresponding author. Email: xinfadeng@163.com

*Astronomical and Astrophysical Transactions*
ISSN 1055-6796 print/ISSN 1476-3540 online © 2006 Taylor & Francis
http://www.tandf.co.uk/journals
DOI: 10.1080/10556790601033015

analysis of photometric red shifts of galaxies in the field of GRB 000210, Gorosabel *et al.* [8] found that there is no obvious concentration of galaxies around the host. In another case, the afterglow of GRB 980613 was located close to a very compact object inside a complex region consisting of star-forming knots and/or interacting galaxy fragments [9, 10]. If these host galaxies are associated with the underlying large-scale structure of the Universe, then they should show similar galaxy clustering properties of normal galaxies. Bornancini *et al.* [11] analysed cross-correlation functions between GRB hosts and surrounding galaxies. Their results indicated that GRB host galaxies do not reside in high-galaxy-density environments; the host–galaxy cross-correlations show a relatively low amplitude. This suggested that the star formation events associated with GRBs occur in particularly low-density environments, a result that is supported by the fact that objects formed in global underdense regions are expected to be biased towards low luminosities, consistent with GRB hosts' characteristics [12].

In this paper, we analyse the local luminous red galaxy (LRG) density surrounding each burst in the *Burst and Transient Source Experiment (BATSE) Current GRB Catalog*. Because few bursts have red-shift data, we calculate only the two-dimensional surface density of LRGs surrounding each burst. Our paper is organized as follows. In section 2, we describe the data to be used. In section 3, we discuss the positional errors of GRBs. In section 4, we analyse the local density of LRGs surrounding bursts. Finally, in section 5, we dicuss and summarize our main results.

## 2. Data

### 2.1 *The galaxy sample*

The Sloan Digital Sky Survey (SDSS) [13] is one of the largest astronomical surveys to date. The SDSS was designed in scope and systematic control to permit the study of galaxy clustering over a wide range of scales and galaxy properties. Galaxy spectroscopic target selection proceeds by two algorithms. The primary sample [14], referred to here as the MAIN sample, targets galaxies brighter than $r < 17.77$ ($r$-band apparent Petrosian magnitude). This sample has a median red shift of 0.10 and few galaxies beyond $z = 0.25$. The LRG algorithm [15] selects galaxies up to $r < 19.5$ that are likely to be luminous early types at red shifts up to about 0.5, using colour–magnitude cuts in $g$, $r$ and $i$. The selection is extremely efficient, and the red-shift success rate is very high. In detail, there are two sections of the LRG algorithm, known as cut I and cut II and described in [15].

The SDSS sky coverage can be separated into three regions: north of the Galactic plane, one region at the celestial equator and another at high declination; south of the Galactic plane, a set of three stripes near the equator. Each of these areas covers a wide range of survey longitudes. We download data from the Catalog Archive Server of Sloan Digital Sky Survey Data Release 3 (SDSS DR3) [16] using the SDSS SQL Search (http://www.sdss.org/) and select from it 26 481 LRGs (with the SDSS flag Primtarget_Galaxy_Red, the red-shift confidence level $z_{\rm conf} > 0.95$ and the red-shift region $0.2 \leqslant z \leqslant 0.4$) and construct our LRG sample.

### 2.2 *The GRB Catalog*

We used the *BATSE Current GRB Catalog*, ending with the trigger number 8121, which occurred on 26 May 2000 (http://f64.nsstc.nasa.gov/batse/grb/catalog/current/). The *BATSE Current GRB Catalog* includes the following: the basic table containing basic

information about bursts (e.g. burst direction) (number of events, 2702); the flux and fluence table containing the peak fluxes on the 64 ms, 256 ms and 1.024 s trigger timescales, and fluences in four energy channels for each burst (number of events, 2135); duration table giving the durations required for integration of 50% and 90% of the burst fluence for each burst (number of events 2041). $T_{50}$ and $T_{90}$ are the burst durations. $T_{90}$ is the time interval in which the integrated counts from the burst increases from 5% to 95% of the total counts; $T_{50}$ is similarly defined (from 25% to 75% of the total counts). According to $T_{90}$, the *GRB Catalog* can be separated into long bursts ($T_{90} \geqslant 2$ s) and short bursts ($T_{90} < 2$ s): number of long bursts, 1540; number of short bursts, 497; an additional four bursts have no position data. The peak flux is defined as the maximum flux in photons per square centimetre per second, integrated over 50–300 keV in energy, and integrated over 64 ms, 256 ms or 1024 ms. According to the peak flux on the 64 ms time scale, we also separate the *GRB Catalog* into strong bursts (peak flux, greater than 3.0) and weak bursts (peak flux, less than 3.0): number of strong bursts, 590; number of weak bursts, 1543; an additional two bursts have no position data.

## 3. The positional errors of gamma-ray bursts

BATSE events are not well localized in the sky. Positional errors are of two types: statistical and systematic. Statistical errors $\sigma_{\rm stat}$ are recorded in the *BATSE GRB Catalog*, range from a fraction of a degree to 30° and are believed to be Gaussian. Systematic errors $\sigma_{\rm sys}$ were analysed using the revised *4B Catalog* [17] and were found to have a more extended tail than Gaussian. For our purposes the approximation used for the *3B Catalog* will suffice; we assume the systematic error distribution to be a Gaussian such that 68% of the events have systematic errors of not more than 1.6°. Assuming that statistical and systematic errors are independent, the total error is defined as $\sigma_{\rm tot} = (\sigma_{\rm stat}^2 + \sigma_{\rm sys}^2)^{1/2} = (\sigma_{\rm stat}^2 + 1.6^2)^{1/2} (\sigma_{\rm sys} = 1.6°)$. The total error distribution of 2702 bursts is plotted in figure 1. The peak of the total error distribution is at about 2°.

In order to explore the error distribution properties of bursts of different types, we plot the total error distributions of strong and weak bursts in figures 2(a) and (b), respectively and those of short and long bursts in figures 3(a) and (b), respectively. We notice that the total errors of strong and long bursts are small on the average, while those of weak and short bursts are large on the average.

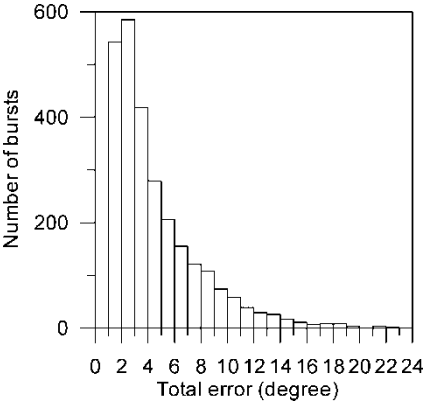


Figure 1. The total error distribution of 2702 bursts for the basic table.

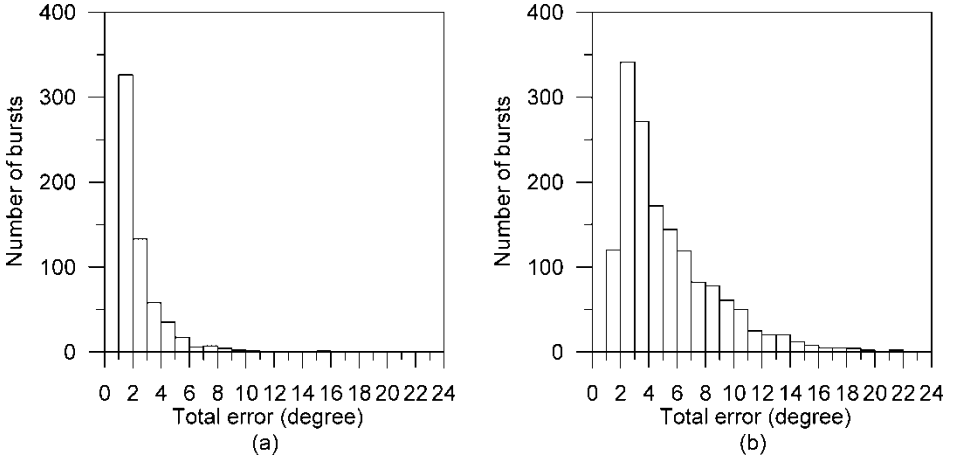


Figure 2. The total error distributions for (a) strong bursts and (b) weak bursts.

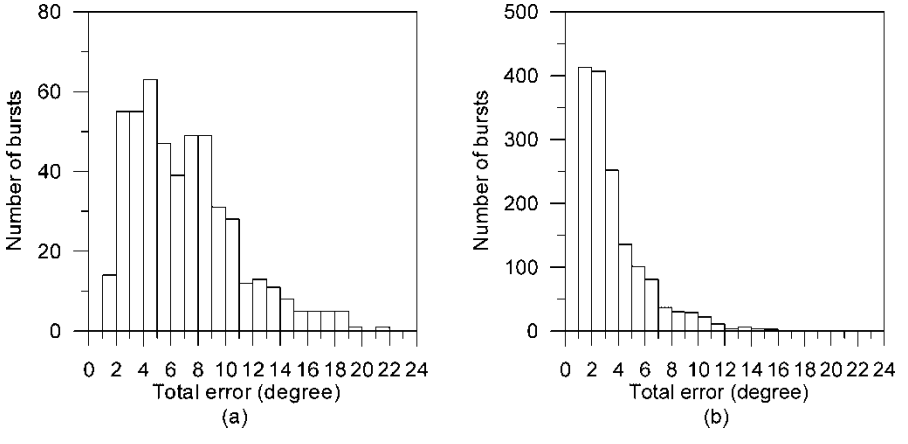


Figure 3. The total error distributions for (a) short bursts and (b) long bursts.

## 4. The local density of luminous red galaxies around bursts

According to the analyses above, we define an angular radius error of 2° and analyse the local surface density of LRGs within this angular radius error region surrounding each burst. The spectroscopic area for SDSS DR3 is 4188 deg$^2$. The average surface density of LRGs in this area is about 6.3 LRGs per square degree. If we calculate the density of LRGs within a certain angular radius region surrounding bursts, the density of LRGs surrounding bursts on the edge of the SDSS sky coverage becomes apparently small. In order to decrease this edge effect, we analyse only bursts of surface density greater than 4 LRGs per square degree. The total number of bursts according to this condition is 227: the number of strong bursts is 41 and the number of weak bursts is 130, with an additional 56 bursts having no peak flux; the number of long bursts is 124 and the number of short bursts is 38, with an additional 65 bursts having no duration. Figure 4 illustrates the distribution of the local surface density of LRGs for 227 bursts. If the edge effect is considered, we think that the surface density of LRGs surrounding most bursts approaches the average surface density (6.3 LRGs per square degree). So we can

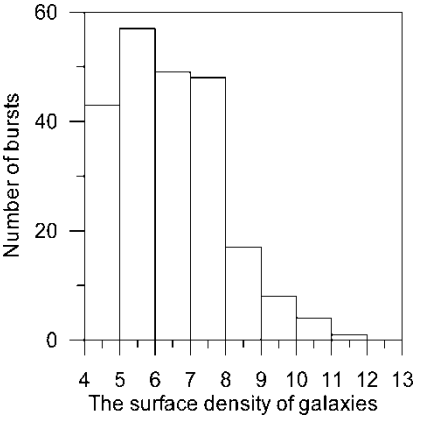


Figure 4. The distribution of the surface densities of LRGs for 227 bursts.

tentatively conclude that there is no correlation between the local density of LRGs and the presence of bursts.

We further analyse the red-shift distribution of LRGs surrounding bursts which have a higher local surface density of LRGs. For this purpose, we select 30 bursts having a high local surface density of LRGs and analyse the red-shift distribution of LRGs surrounding these bursts. Only in a few bursts (e.g. trigger number 7952) do LRGs have a dense red-shift distribution. Figure 5 shows a plot of the red-shift distribution of LRGs surrounding trigger number 7952, but most bursts do not have this property. Figure 6 shows the red-shift distribution of LRGs surrounding trigger number 2713. Around this burst, there is the highest local surface density of LRGs (11.38 LRGs per square degree), but apparently there is no dense red-shift distribution of LRGs. This demonstrates that, even if some bursts have a higher local surface density of LRGs, they often do not reside in a high-density region of LRGs in three-dimensional space. So we further conclude that there is no correlation between the local density of LRGs and the presence of bursts.

We have constructed an 'accurate' subclass of the GRB sample (which contains 538 GRBs) with a good positional accuracy, namely a subclass for which the positional error $\sigma_{\rm tot}$ satisfies $\sigma_{\rm tot} < 2^\circ$. Most bursts of this subclass are long (number of long bursts, 410; number of short bursts, 13; other bursts have no duration). We calculate the local surface density of LRGs

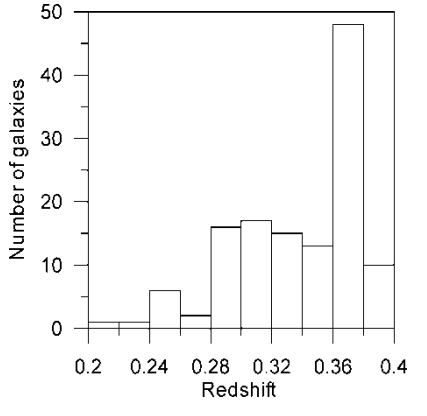


Figure 5. The red-shift distribution of LRGs surrounding trigger number 7952.

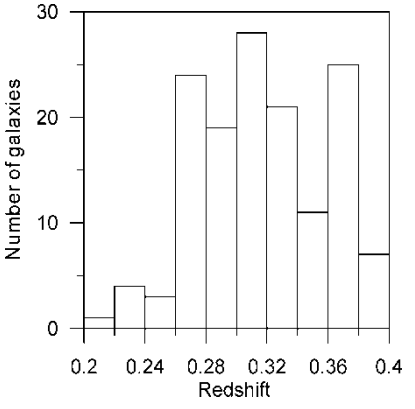


Figure 6. The red-shift distribution of LRGs surrounding trigger number 2713.

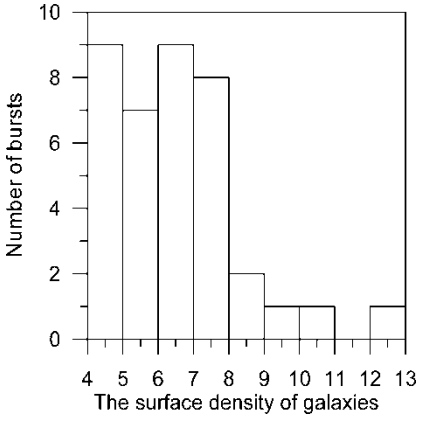


Figure 7. The distribution of surface densities of LRGs for 38 bursts in the 'accurate' subclass.

within an angular radius of less than 1.5° surrounding each burst in the 'accurate' subclass. As in the above analysis, we consider only bursts of surface density greater than 4 LRGs per square degree. The total number of bursts according to this condition in the 'accurate' subclass is 38. Figure 7 shows the distribution of the surface density of LRGs for these 38 bursts. If some bursts are considered to have the edge effect, the surface density of LRGs surrounding most bursts in the 'accurate' subclass approaches the average surface density of LRGs (6.3 LRGs per square degree). We further analyse the red-shift distribution of LRGs surrounding five bursts having the highest local surface densities of LRGs. Finally, we conclude that there is no correlation between the local density of LRGs and the bursts in the 'accurate' subclass.

## 5. Discussion and conclusions

The study of the characteristics of the physical environment surrounding GRBs will be beneficial to the understanding of the origin of these events. So we have analysed the correlation between the local density of LRGs and the presence of GRBs. We use an LRG sample in SDSS DR3 and the *BATSE Current GRB Catalog*. The LRG sample is limited to the red-shift region $0.2 \leqslant z \leqslant 0.4$ and includes 26 481 LRGs. The main results can be summarized as follows.

(1) BATSE events are not well localized in the sky. Positional errors contain two parts: statistical and systematic. The total error is defined as $\sigma_{\rm tot} = (\sigma_{\rm stat}^2 + \sigma_{\rm sys}^2)^{1/2} = (\sigma_{\rm stat}^2 + 1.6^2)^{1/2} (\sigma_{\rm sys} = 1.6^\circ)$. The peak of the total error distribution is at about $2^\circ$. We futher explore the error distribution properties of bursts of different types. The results show that the total errors of strong and long bursts are small on the average, while those of weak and short bursts are large on the average.

(2) According to positional error analyses, we select an angular radius of $2^\circ$ and analyse the local surface density of LRGs within this angular radius region surrounding each burst. If the edge effect is considered, we find that the surface density of LRGs surrounding most bursts approaches the average surface density of LRGs (6.3 LRGs per square degree). This result demonstrates that there is no correlation between the local density of LRGs and the presence of bursts.

(3) We further analyse the red-shift distribution of LRGs surrounding bursts having a higher local surface density of LRGs. LRGs have a dense red-shift distribution around a few bursts, but most bursts do not have this distinguishing feature This demonstrates that, even if some bursts have a higher local surface density of LRGs, they often do not reside in a high-density region of LRGs in three-dimensional space.

(4) In order to explore the local density of LRGs surrounding bursts within a smaller angular radius region, we have constructed an 'accurate' subclass of the GRB sample (which contains 538 GRBs) with a good positional accuracy ($\sigma_{\rm tot} < 2^\circ$). It mainly consists of long bursts. We analyse the local surface density of LRGs within an angular radius of less than $1.5^\circ$ surrounding each burst for the 'accurate' subclass. The analysed results further testify to the above conclusion.

## References


[1] J. van Paradijs, C. Kouveliotou and R.A.M.J. Wijers, A. Rev. Astron. Astrophys. **38** 379 (2000).
[2] D. Eichler, M. Livio, T. Piran and D.N. Schramm, Nature **340** 126 (1989).
[3] R. Mochkovitch, M. Hernanz, J. Isern *et al.*, Nature **361** 236 (1993).
[4] S.E. Woosley, Astrophys. J. **405** 273 (1993).
[5] B. Paczy'nski, Astrophys. J. **494** L45 (1998).
[6] A.I. MacFadyen and S.E. Woosley, Astrophys. J. **524** 262 (1999).
[7] J.P.U. Fynbo, P. Moller, B. Thomsen *et al.*, Astron. Astrophys. **388** 425 (2002).
[8] J. Gorosabel, L. Christensen, J. Hjorth *et al.*, Astron. Astrophys. **400** 127 (2003).
[9] J. Hjorth, B. Thomsen, S.R. Nielsen *et al.*, Astrophys. J. **576** 11 (2002).
[10] S.G. Djorgovski, J.S. Bloom and S.R. Kulkarni, Astrophys. J. **591** L13 (2003).
[11] C.G. Bornancini, H.J. Martnez, D.G. Lambas *et al.*, Astrophys. J. **614** 84 (2004).
[12] E. Le Floch, P.A. Duc, I.F. Mirabel *et al.*, Astron. Astrophys. **400** 499 (2003).
[13] D. York, J. Adelman, J.E. Jr. Anderson *et al.*, Astron. J. **120** 1579 (2000).
[14] M.A. Strauss, D.H. Weinberg, R.H. Lupton *et al.*, Astron. J. **124** 1810 (2002).
[15] D.J. Eisenstein, J. Annis, J.E. Gunn *et al.*, Astron. J. **122** 2267 (2001).
[16] K. Abazajian, J.K. Adelman-McCarthy, M.A. Agueros *et al.*, Astron. J. **129** 1755 (2005).
[17] W.S. Paciesas, C.A. Meegan, G.N. Pendleton *et al.*, Astrophys. J., Suppl. Ser. **122** 465 (1999).